ORIGINAL RESEARCH PAPER

Computer Science

PERFORMANCE ENHANCEMENT OF BLDC MOTOR DRIVES TO IMPROVE THE PRODUCTION EFFICIENCY OF LARGE SCALE INDUSTRIES.

KEY WORDS: PMBLDC Motor, simulation and modeling, speed control.

Dr.V M Varatharaju

Faculty, Engineering Department, Ibra college of Technology, Ibra, Sultanate of Oman.

ABSTRACT

Permanent magnet brushless dc motor (PMBLDCM) drives are persistently picking up ubiquity moving control applications. Right now mathematical model of the drive framework is created to break down its exhibition. The structured trapezoidal BLDC motor based drive framework has the shut circle speed control, in which PI algorithm is embraced and the position assurance is done through hysteresis current control. The nonlinear reenactment model of the BLDC motor drive framework with PI control based is reproduced in the MATLAB/Simulink stage. The reenacted outcomes in electromagnetic torque and rotor speed are given. The conversations could be a decipherable content on the activity, displaying, and control of BLDCM for graduate understudies concentrating electric drives and control just as rehearsing motors in businesses.

1. INTRODUCTION

Permanent magnet motor is one type of synchronous motor, which can be worked in perilous barometrical condition and at high speeds because of the nonattendance of brushes (Duane C.Hanselman, 1994). Parmanent magnet motors with trapezoidal back EMF and sinusoidal back EMF have a few points of interest over other motor types. Most outstandingly, (contrasted with dc motors) they are lower upkeep because of the disposal of the mechanical commutator and they have a powerful thickness which makes them perfect for high-torque-to weight proportion applications (T.J.E.Miller, 1989). Contrasted with acceptance machines, they have lower dormancy considering quicker powerful reaction to reference directions. Additionally, they are increasingly productive because of the parmanent magnets which brings about for all intents and purposes zero rotor misfortunes (R.Krishnan, 2001). Parmanent magnet brushless dc (PMBLDC) motors could become genuine contenders to the enlistment motor for servo applications. The PMBLDC motor is getting well known in different applications due to its high productivity, high force factor, high torque, straightforward control and lower upkeep (P. Pillay and R. Krishnan, 1989). The significant burden with perpetual magnet motors is their greater expense and generally higher intricacy presented by the force electronic converter used to drive them. The additional unpredictability is clear in the improvement of a torque/speed controller (P. Pillay and R. Krishnan, 1988).

The magnetization directions and intensities are analyzed using finite element analysis with a detailed magnetization procedure for ferrite bonded magnets used in inner-rotor type BLDC motors (In-Soung Jung *et al*, 2001). The effect of stator resistance on average-value modeling of electromechanical systems consisting of BLDC motor and 120-degree inverter systems, including commutation current has been presented (Qiang Han *et al*, 2007). It is shown that the model becomes more accurate both in time and frequency domains for the motors with large stator resistance (small electrical time constant of the stator winding) typically operate with small commutation angle. *Bhim singh, B P singh and K Jain* have proposed a digital speed controller for BLDCM and implemented in a digital signal processor (Bhim singh *et al*, 2002). Later schemes have been developed to extract the rotor position and the speed of BLDC motor by Extended Kalman Filter (EKF) (R.Dhaouadi, 1991). The Hall Effect sensors have been successfully adapted to sense the rotor position for every 60 degree electrical (T.Sebastian *et al*, 1989, M.Lajoie-Mazenc *et al*, 1985).

Modeling and simulation of electromechanical systems with BLDC drives are essential steps at the design stage of such systems. For the purposes of stability analysis and controller design, it is often desirable to investigate the large-signal transients and small-signal characteristics of the system. Simulation studies are also often performed many times to achieve the required design goals. In this study, the nonlinear simulation model of the BLDC motors drive system with proportional-integral (PI) control based on MATLAB/Simulink platform is presented. The simulated results in terms of electromagnetic torque and rotor speed are given.

2. Narrative of PMBLDCM Drive

Fig.1 shows the typical BLDC motor controlled by an inverter. The BLDC motor does not have brush and many problems resulting from mechanical wear of brushes. The commutator function is improved by changing the position of rotor and stator. To alternate the function of brushes and commutator, the BLDC motor requires an inverter and a position sensor that detects rotor position for proper commutation of current. i.e. Unlike a brushed DC motor, the commutation of a BLDC motor is controlled electronically.

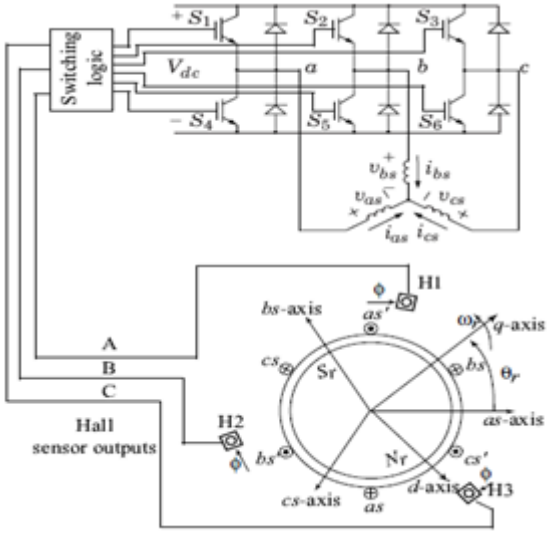

Fig.1 BLDC Motor controlled by the inverter

Typical Hall-sensor-controlled BLDC motors, such as the one considered in this paper, is very common. The inverter converts a dc source voltage into 3-phase ac voltages with frequency corresponding to the rotor position and speed. The inverter may operate using 180 or 120 degree commutation methods, but the latter method is particularly common due to its simplicity. This paper focuses on typical Hall-sensor controlled VSI-driven BLDC motors, where the inverter operates using 120-degree commutation method. Rotor position is sensed by Hall Effect sensors embedded into the

stator which gives the sequence of phases. Whenever the rotor magnetic poles pass near the Hall sensors, they give a high/low signal, indicating the N or S pole is passing near the sensors. The three Hall sensors, *H*1, *H*2, and *H*3, are used to detect the rotor position. The logical signals from the Hall sensors *H*1, *H*2, *H*3 are used to control the inverter switches (S_1 – S_6). These Hall sensor signals partition the rotation circle into six 60-degree switching intervals (SI), which are numbered I–VI and shown in Fig.2. To rotate the BLDC motor, the stator windings should be energized in a sequence. Based on the combination of these three Hall sensor signals, the exact sequence of commutation can be determined.

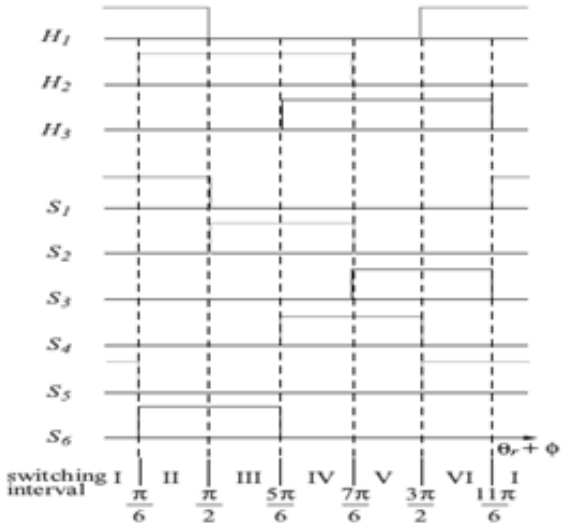

Fig.2 Switching signals

2.1 Closed Loop Control

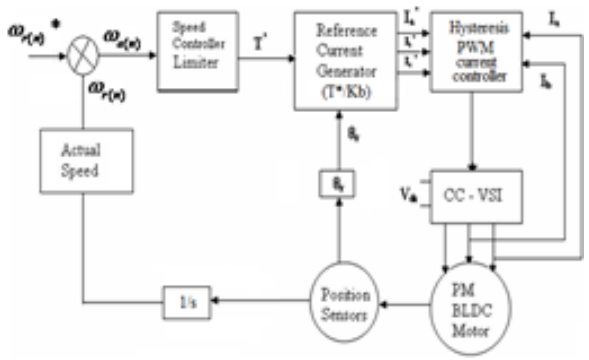

Fig. 3 PMBLDC motor drive system

Fig.3 describes the basic building blocks of the PMBLDCM drive system. The drive consists of speed controller, reference current generator, pulse width modulation (PWM) current controller, position sensor, the motor and a IGBT based voltage source inverter (CC-VSI). The speed of the motor is compared with its reference value and the speed error is processed in PI speed controller. The output of this controller is considered as the reference torque. A limit is put on the speed controller output depending on permissible maximum winding currents. The reference current generator block generates the three phase reference currents (i_a , i_b , ic) using the limited peak current magnitude decided by the controller and the position sensor.

The reference currents have the shape of quasi-square wave in phase with respective back emfs to develop constant unidirectional torque as shown in Fig.4. The PWM current controller regulates the winding currents (i_a, i_b, i_c) within the small band around the reference currents (i_a , i_b , i_c). The motor currents are compared with the reference currents and the switching commands are generated to drive the power switches.

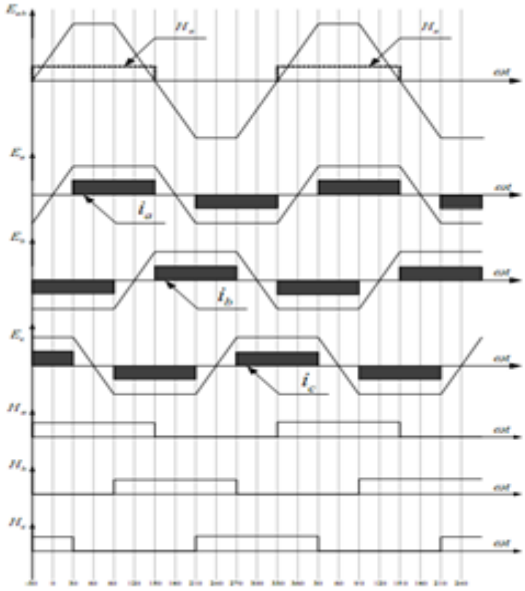

Fig.4 Back EMF pattern and reference current generation

The PI controller is widely used in industry due to its ease in design and simple structure. The rotor speed $\omega_r(n)$ is compared with the reference speed $\omega_r(n)^*$ and the resulting error is estimated at the n[th] sampling instant as:

$$\omega_e(n) = \omega_r(n)^* - \omega_r(n) \qquad (1)$$

The new value of torque reference is given by

$$T(n) = T(n-1) + K_P\omega_e(n) - \omega_e(n-1) + K_I\omega_e(n) \qquad (2)$$

Where, 'ω_e(n−1)' is the speed error of previous interval, and 'ω_e(n)' is the speed error of the working interval. K_P and K_I are the gains of proportional and integral controllers respectively. By using Ziegler Nichols method the K_P and K_I values are determined (A.Rubai *et al*, 1992).

2.2 Reference Current Generator

The magnitude of the reference current (I^*) is determined by using reference torque (T^*) and the back emf constant (K_b);

$$I^* = \frac{T^*}{K_b}$$

(P.C.K.Luk *et al*, 1994). Depending on the rotor position, the reference current generator block generates three-phase reference currents (i_a^*, i_b^*, i_c^*) considering the value of reference current magnitude as I^*, $-I^*$ and zero. The reference current generation is explained in the Table.1.

Table 1. Rotor position signal Vs reference current

Rotor Position Signal θ_r	Reference Currents (i_a^*, i_b^*, i_c^*)		
θ° - 60°	I*	–I*	0
60° - 120°	I*	0	–*
120° -180°	0	I*	–I*
180° - 240°	–I*	I*	0
240° - 300°	–I*	0	I*
300° - 360°	0	–I*	I*

2.3 PWM Current Controller

The PWM current controller contributes to the generation of the switching signals for the inverter switches. The switching logic is formulated as given below.

If $i_a < (i_a^*)$ switch 1 ON and switch 4 OFF
If $i_a > (i_a^*)$ switch 1 OFF and switch 4 ON

If $i_b < (i_b^*)$ switch 3 ON and switch 6 OFF
If $i_b > (i_b^*)$ switch 3 OFF and switch 6 ON
If $i_c < (i_c^*)$ switch 5 ON and switch 2 OFF
If $i_c > (i_c^*)$ switch 5 OFF and switch 2 ON

3. Modeling

3.1 Back EMF

The phase back emf in the PMBLDC motor is trapezoidal in nature and also a function of the speed (ω_r) and rotor position angle (θ_r) as shown in Fig.5. The normalized function of back emfs is shown in Fig.5. From this, the phase back emf (e_{an}) can be expressed as

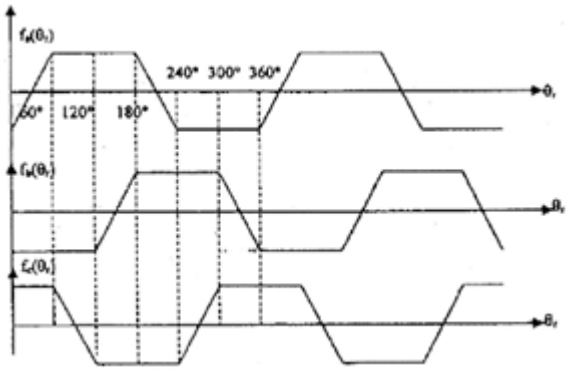

Fig. 5 Components of back EMF

$$f_a(\theta_r) = E \qquad 0^0 < \theta_r < 120^0$$
$$f_a(\theta_r) = (6E/\pi)(\pi - \theta_r r) - E \qquad 120^0 < \theta_r < 180^0$$
$$f_a(\theta_r) = -E \qquad 180^0 < \theta_r < 300^0$$
$$f_a(\theta_r) = (6E/\pi)(\theta_r r - 2\pi) + E \qquad 300^0 < \theta_r < 360^0$$

(3) Where, brE=K ωand e_{an} can be described by E and normalized back emf function $f_a(\theta_r)$ [$e_{an} = E\, f_a(\theta_r)$]

The back emf functions of other two phases (e_{bn} and e_{cn}) can also be determined in similar way using E and the normalized back emf function $f_b(\theta_r)$ and $f_c(\theta_r)$.

4. PMBLDC Motor and Inverter

The PMBLDC motor is modeled in the 3-phase abc frame. The general volt-ampere equation for the circuit shown in the Fig.6 can be expressed as:

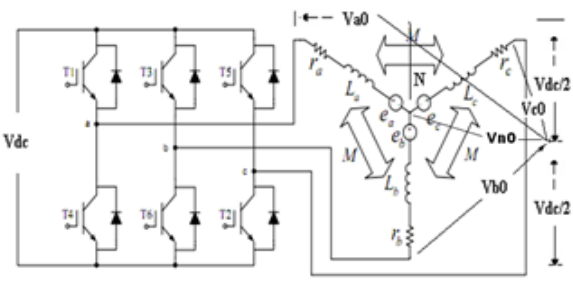

Fig.6 Inverter circuit with PMBLDCM drive

(4)

$$V_{an} = Ri_a + p\lambda_a + e_{an}$$

(5)

$$V_{bn} = Ri_b + p\lambda_b + e_{bn}$$

(6)

$$V_{cn} = Ri_c + p\lambda_c + e_{cn}$$

Where, V_{an}, V_{bn} and V_{cn} are phase voltages and may be defined as:

$$V_{an} = V_{a0} - V_{n0},$$
$$V_{bn} = V_{b0} - V_{n0}, \text{ and}$$
$$V_{c0} = V_{c0} - V_{n0}.$$

(7)

Where V_{a0}, V_{b0}, V_{c0} and V_{n0} are three phase and neutral voltages with respect to the zero reference potential at the mid-point of dc link (0) shown in the Fig.6. R is the resistance per phase of the stator winding, p is the time differential operator, and e_{an}, e_{bn} and e_{cn} are phase to neutral back emfs. The λ_a, λ_b and λ_c are total flux linkage of phase windings a, b and c respectively. Their values can be expressed as:

$$\lambda_a = L_S i_a - M(i_b + i_c)$$

(8)

$$\lambda_b = L_S i_b - M(i_a + i_c)$$

(9)

$$\lambda_c = L_S i_c - M(i_a + i_b)$$

(10)

Where, 'Ls' and 'M' are self and mutual inductances respectively.

The PMBLDC motor has no neutral connection and hence this results in,

$$i_a + i_b + i_c = 0$$

(11) Substituting (11) in (8), (9) and (10), the flux linkages are obtained.

$$\lambda_a = i_a(L_S + M),$$
$$\lambda_b = i_b(L_S + M), \text{ and}$$
$$\lambda_c = i_c(L_S + M)$$

(12) By substituting (12) in volt-ampere relations (4)-(6) and rearranging these equations in a current derivative of statespace form, gives,

$$pi_a = 1/(L_S + M)(V_{an} - Ri_a - e_{an})$$

(13)

$$pi_b = 1/(L_S + M)(V_{bn} - Ri_b - e_{bn})$$

(14)

$$pi_c = 1/(L_S + M)(V_{cn} - Ri_c - e_{cn})$$

(15)

The developed electromagnetic torque may be expressed as

$$T_e = (e_{an}i_a + e_{bn}i_b + e_{cn}i_c)/\omega_r$$

(16) Where, 'ωr' is the rotor speed in electrical rad/sec. After substitution of the back emfs in normalized form, the developed torque is given by

$$T_e = K\{f_a(\theta_r)i_a + f_b(\theta_r)i_b + f_c(\theta_r)i_c\}$$

(17) The mechanical equation of motion in speed derivative form can be expressed as:

$$p\omega_r = (P/2)(T_e - T_L - B\omega_r)/J$$

(18) Where, 'P' is the number of poles, 'TL' is the torque load in N-m, 'B' is the frictional coefficient in Nm/rad, and 'J' is the moment of inertia in kg-m^2.

The derivative of the rotor position (θr) in state space form is expressed as:

$$p\theta_r = \omega_r$$

(19)

The potential of the neutral point with respect to the zero potential (v_{n0}) is required to be interpreted properly to avoid the imbalance in applied phase voltages.

This can be obtained by substituting (7) in (4) to (6) and adding them together to give

$$V_{a0} + V_{b0} + V_{c0} - 3V_{n0} = R(i_a + i_b + i_c) + (L_S + M)(pi_a + pi_b + pi_c) + (e_{an} + e_{bn} + e_{cn})$$

(20) Substituting (11) in (20) results in

$$V_{a0} + V_{b0} + V_{c0} - 3V_{n0} = (e_{an} + e_{bn} + e_{cn})$$
$$\Rightarrow V_{n0} = [V_{a0} + V_{b0} + V_{c0} - (e_{an} + e_{bn} + e_{cn})]/3$$

(21) The set of differential equations viz. (13),(14), (15), (18) and (19) defines the developed model in terms of the variables ia, ib, ic, ωr, and θr for the independent variable, time.

5. Simulation Results

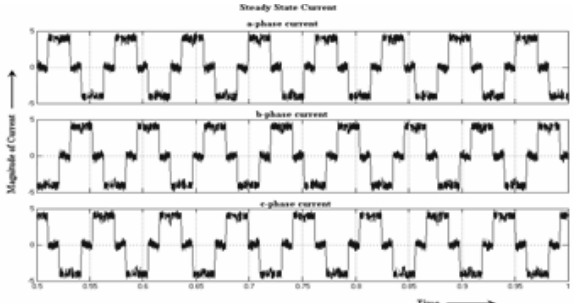

Fig.7 Stator phase currents

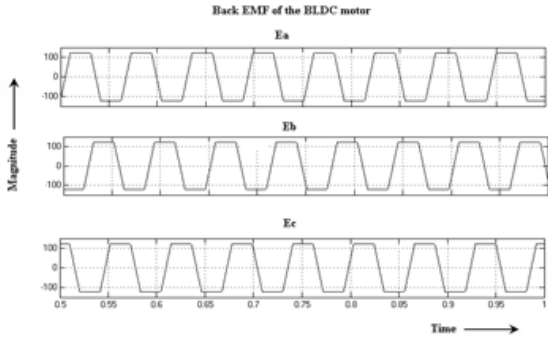

Fig. 8 Trapezoidal back EMF

In this work the drive model with PI speed controller is developed and simulated in order to validate the model and the designed controller. The set of equations representing the model of the drive system is schematized. For conducting the studies and analysis, this paper considers a typical industrial BLDC motor (Arrow Precision Motor Co., LTD) with importance specifications: 2hp, 1500rpm, 4 poles (Refer Appendix). Fig.7-14 shows simulated results

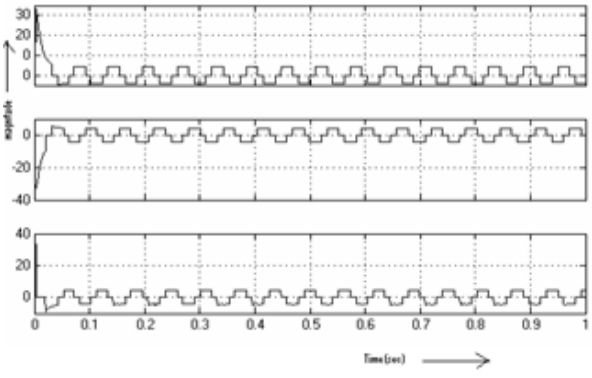

Fig. 9 Reference current waveform

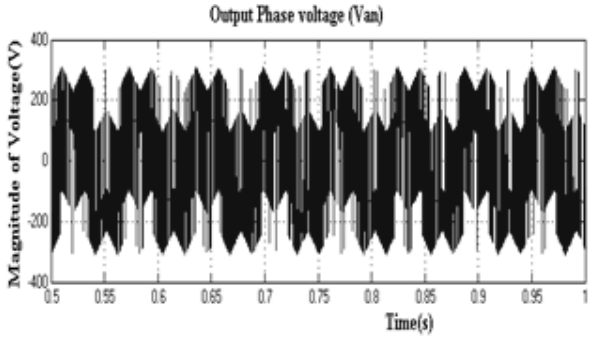

Fig. 10 Representative phase voltage (v_{an})

Fig.7 and Fig.8 show the stator phase currents and back emf respectively. Fig.9 shows the reference current. The typical phase voltage is diagrammed in Fig.10. Fig.11 shows the torque and the speed variations, and the motor speed quickly converges to the reference shortly after startup and recovers very well from the load torque disturbance as well as parameters variation. The moment of inertia value taken for this case is 0.013kg-m^2 and it reaches the steady state torque and speed suddenly at time 0.03seconds. When the moment of inertia is increased to 0.098kg-m^2 it takes 0.28 seconds to reach the steady state as evidenced in Fig.13. From the figure, it is inferred that increasing the moment of inertia will cause the settling time to increase.

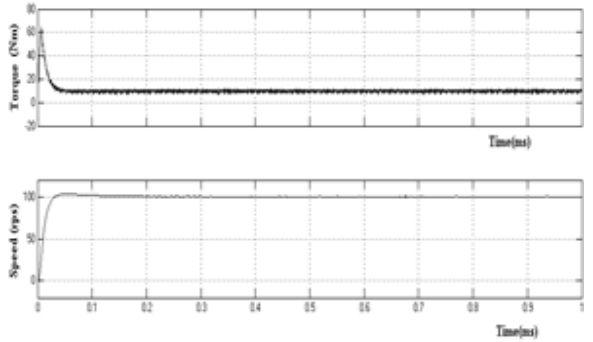

Fig. 11 Torque and speed responses during startup transients

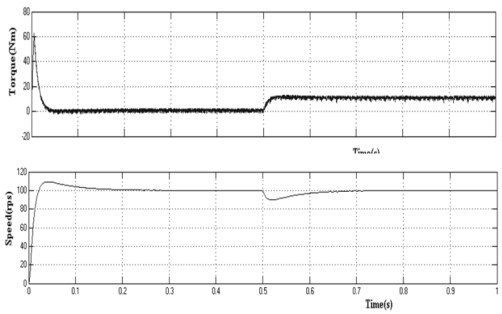

Fig. 12 Torque and speed responses - step input change - moment of inertia 0.013 kg-m^2 (step time 0.5 S)

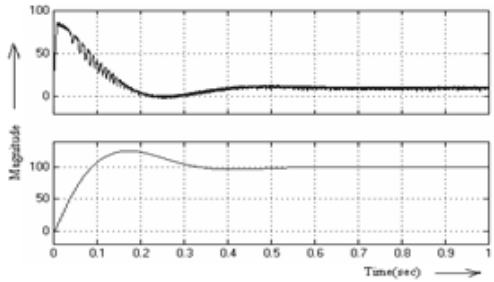

Fig. 13 Torque and speed responses at moment of inertia 0.098 kg-m^2

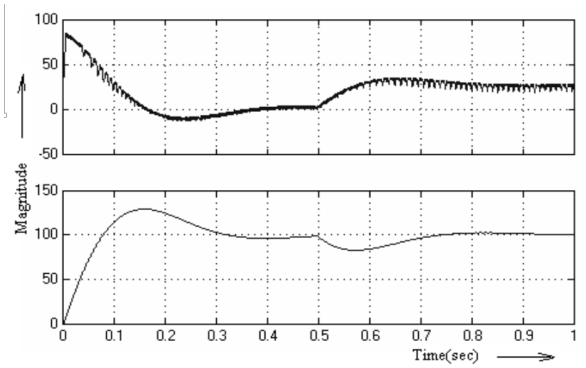

Fig. 14 Torque and speed-Step input with moment of inertia, 0.098 kg-m^2 (step time 0.5 S)

Fig.12 and Fig.14 demonstrate the drive performance with step inertia change. The simulated results show that synchronization of the rotor speed is well done and the average electromagnetic torque is in equilibrium although the dynamic electromagnetic torque is not in equilibrium.

6. CONCLUSION

The nonlinear simulation model of the BLDC motor drive framework with PI control dependent on MATLAB/Simulink stage is exhibited. The control structure has an inward current shut circle and an external speed circle to administer the current. The speed controller manages the rotor development by differing the recurrence of the beat dependent on signal input from the Hall sensors. The presentation of the created PI calculation based speed controller of the drive has uncovered that the calculation devises the conduct of the PMBLDC engine drive framework work acceptably. Current is directed inside band by the hysteresis current controller. And furthermore by differing the snapshot of dormancy see that expansion right now it expands simulation time to arrive at the consistent state esteem.

Thusly, the created controller has powerful speed qualities against parameters and idleness varieties. In this way, it very well may be adjusted speed control for superior BLDC motor.

REFERENCES

1. Duane C.Hanselman, "Brushless Permanent-Magnet Motor Design", McGraw-Hill, Inc., New York, 1994.
2. T.J.E.Miller, "Brushless Permanent Magnet and Reluctance Motor Drives", Oxford Science Publication, UK, 1989.
3. R.Krishnan, "Electric Motor Drives: Modeling, Analysis, and Control, Prentice-Hall, Upper Saddle River, NJ, 2001.
4. P. Pillay and R. Krishnan, "Modeling, simulation, and analysis of permanent Magnet motor drives. Part II: The brushless dc motor drive," *IEEE Transactions on Industry Applications*, vol.IA-25, no.2, pp.274–279, Mar./Apr. 1989.
5. P. Pillay and R. Krishnan, Modeling of permanent magnet motor drives*", IEEE Transactions on Industrial Electronics*, vol.35, no.4, pp-537 – 541, Nov. 1988.
6. In-Soung Jung, Ha-Gyeong Sung, Yon-Do Chun, and Jin-Hwan Borm, "Magnetization Modeling of a Bonded Magnet for Performance Calculation of Inner-Rotor Type BLDC Motor", *IEEE Transactions on Magnetics*, vol.37, no.4, pp.2810-2813, July 2001.
7. Qiang Han, Hee-Sang Ko, Juri Jatskevich, "Effect of Stator Resistance on Average-Value Modeling of BLDC Motor 120-Degree Inverter Systems", *Proceeding of International Conference on Electrical Machines and Systems (ICEMS07)*, pp.481-486, Oct.8-11, Seoul, Korea, 2007.
8. Bhim singh, B.P.Singh and (Ms) K.Jain, "Implementation of DSP Based Digital Speed Controller for Permanent Magnet Brushless dc Motor", *Journal of The Institution of Motorers (India)*, vol.84, pp-16-21, June 2003.
9. R.Dhaouadi, N.Mohan, and L.Norum, "Design and implementation of an extended Kalman filter for the state estimation of a permanent magnet synchronous motor," *IEEE Transactions on Power Electronics*, vol.6, pp.491-497, July 1991.
10. T.Sebastian and G.R.Slemon, "Transient Modeling and Performance of Variable Speed Permanent Magnet Motors." *IEEE Transactions on Industry Applications*, vol-25, no.1, pp.101, January/February 1989.
11. M.Lajoie-Mazenc, C.Villanueva, and J.Hector, "Study and implementation of a hysteresis controlled inverter on a permanent magnet synchronous machine," *IEEE Transactions on Industry Applications*, vol. IA-21, no.2, pp.408-413, March/April 1985.
12. A.Rubai and R.C.Yalamanchi, "Dynamic Study of an Electronically Brushless dc Machine via Computer Simulations." *IEEE Transactions on Energy Conversion,* vol.7, no.1, pp.132-138, March 1992.
13. P.C.K.Luk and C.K.Lee, "Efficient Modeling for a Brushless dc Motor Drive", *20th International Conference on Industrial Electronics, Control and Instrumentation (IECON'94)*, vol.1, pp.188-191, Spet.5-9, 1994.